



Exact Solutions for Real and Complex Nonlinear Partial Differential Equations in Engineering Using a Modified Homotopy Perturbation Method

Osama Alkhazaleh,^{1,*} James Nergard² and Cam Shepherd²

Abstract

Nonlinear partial differential equations (PDEs) play a fundamental role in modeling complex phenomena in physics and engineering. However, solving them analytically and numerically remains challenging due to divergence, slow convergence, and computational inefficiency. This study implements a refined variation of the homotopy perturbation method (HPM), termed the modified homotopy perturbation method (MHPM), to improve accuracy and stability in solving nonlinear PDEs. The motivation behind this work stems from the need for a more efficient and reliable approach, particularly for equations where traditional methods fail to yield convergent or computationally efficient solutions. By integrating Padé approximants and Laplace transforms, MHPM enhances convergence, reduces computational effort, and maintains high precision. To validate its effectiveness, the method is applied to several well-known nonlinear equations, including the nonlinear gas dynamics equation, nonlinear wave-like equation, cubic complex Ginzburg-Landau equation, one- and two-dimensional nonlinear Schrödinger equations, and higher-order nonlinear PDEs that are fundamental in fluid dynamics, wave propagation, quantum mechanics, and mathematical modeling. A systematic comparison confirms that MHPM not only improves solution accuracy but also provides a practical, computationally efficient alternative to conventional analytical and numerical techniques. The results underscore its potential for multi-dimensional and time-dependent PDEs, reinforcing its value in nonlinear system analysis across theoretical and applied sciences.

Keywords: Nonlinear partial differential equations; Convergence and computational efficiency; Multi-physics modeling.

Received: 28 January 2025; Revised: 07 April 2025; Accepted: 25 May 2025.

Article type: Research article.

1. Introduction

Nonlinear partial differential equations (PDEs) are central to numerous theoretical and practical advancements, serving as essential tools for modeling complex phenomena in physics, engineering, and applied mathematics. From capturing the intricate dynamics of turbulent fluids to modeling wave propagation in optical fibers and quantum systems, nonlinear PDEs provide a mathematical framework for describing processes that are both fundamental and ubiquitous. However, solving these equations remains a significant challenge due to

their nonlinearity, complexity, and, in many cases, the lack of exact solutions.

The importance of nonlinear PDEs extends beyond academia, as they underpin critical applications in fluid dynamics, where they describe the motion of gases and liquids, and in quantum mechanics, where they govern the evolution of wave functions. Additionally, they are integral to wave mechanics, modeling sound and electromagnetic waves, and play a crucial role in engineering applications such as structural analysis and material science. Despite their broad significance, traditional approaches to solving nonlinear PDEs often face limitations in terms of convergence, stability, and computational efficiency.

Although numerous analytical and numerical techniques exist for solving nonlinear PDEs, many are limited by simplifying assumptions, slow convergence, or high computational costs. This study addresses these limitations by employing the modified homotopy perturbation method

¹ Department of Mathematics, Embry-Riddle Aeronautical University-Prescott Campus, Arizona, 86301, USA

² Department of Engineering, Embry-Riddle Aeronautical University-Prescott Campus, Arizona, 86301, USA

*Email: alkhazao@erau.edu; osamaalkhazaleh@gmail.com (O. Alkhazaleh)

(MHPM) to solve highly nonlinear and complex PDEs in both real and complex domains. Rather than modifying MHPM itself, this work expands its application to a broader class of equations, demonstrating its effectiveness in solving problems that conventional methods struggle to resolve. Through a systematic analysis of the method's behavior in diverse cases, this study highlights MHPM's ability to achieve accurate solutions while maintaining computational efficiency. Furthermore, a comparative analysis illustrates how MHPM performs relative to established techniques in solving particularly challenging PDEs.

Over the years, a variety of analytical methods have been proposed to tackle these challenges, including the Adomian decomposition method,^[1] the variational iteration method,^[2] asymptotic methods,^[3] homotopy perturbation method (HPM),^[4] fractional calculus,^[5,6] traveling wave and soliton solutions,^[7,8] bifurcation analysis,^[9] reproducing kernel-based numerical algorithms ^[10,11], and decomposition techniques for fractional and time-fractional PDEs.^[12,13] Among these, HPM has emerged as a powerful tool due to its ability to deliver exact solutions while avoiding discretization, linearization, or reliance on a small parameter. The applicability of HPM has been extensively studied, with convergence analyses confirming its effectiveness in solving a range of problems.^[14] Additionally, refinements such as Hemedi's extension for fractional-order equations in the Caputo sense have further expanded its applications.^[15] However, like other perturbation-based approaches, HPM encounters challenges in achieving reliable convergence, particularly for highly nonlinear or non-ideal problems.^[16-20] These limitations have driven the development of improved techniques to extend HPM's applicability and enhance its performance.

This study builds upon the foundations of HPM and introduces a refined approach, referred to as MHPM.^[21] By incorporating Laplace transforms and Padé approximants into the traditional HPM framework, MHPM addresses key challenges related to convergence and precision. The Laplace transform enhances the method by transforming the series solution into a domain more suitable for analysis, while the Padé approximant constructs a meromorphic function that accelerates convergence and improves stability. The inverse Laplace transform then recovers the solution in its original form, providing an efficient and reliable pathway to exact solutions.

The versatility of MHPM is demonstrated through its application to several pivotal equations, including the nonlinear gas dynamics equation, nonlinear wave-like equation, nonlinear cubic complex Ginzburg-Landau equation, one- and two-dimensional nonlinear Schrödinger equations, and higher-order nonlinear PDEs. These examples are not just theoretical but also serve as fundamental models in fluid dynamics, wave propagation, and quantum mechanics. By providing precise and computationally efficient solutions, MHPM highlights its potential as a valuable tool for advancing the study of nonlinear systems in both theoretical research and

applied sciences.

This paper is structured as follows. Section 2 presents the fundamental concepts underlying HPM and Padé approximants, laying the groundwork for MHPM, along with an exploration of its modifications. Section 3 highlights the efficiency of MHPM through various benchmark cases and real-world scenarios. Section 4 analyzes the outcomes derived from MHPM and evaluates its performance relative to established approaches. Finally, Section 5 concludes with an overview of the findings and their potential impact on advancing research in the field.

2. Basic principles

This section outlines the foundational principles of the HPM and the methodology of Pade approximants, which form the basis of MHPM. For clarity, in this work, the uppercase symbol Ω is used to denote exact solutions, while the lowercase symbol ω represents estimated solutions.

2.1 Homotopy perturbation method

To present the central concept, examine the general form of a differential Eq. (1):

$$L(\Omega) + N(\Omega) - F(v) = 0, v \in R \quad (1)$$

where L, N , and F are a linear operator, a nonlinear operator, and an analytic function, respectively.

The HPM constructs a homotopy in the following Eqs. (2) and (3).

$$H(\omega, p) = (1 - p)[L(\omega) - L(\Omega_0)] + p[A(\omega) - F(v)] = 0 \quad (2)$$

$$H(\omega, p) = L(\omega) - L(\Omega_0) + pL(\Omega_0) + p[N(\omega) - F(v)] = 0 \quad (3)$$

where $\omega(v, p): R \times [0,1] \rightarrow \mathbb{R}$, p is the embedding parameter, and Ω_0 is an initial approximation satisfying the boundary conditions. When $p = 0$, Eq. (4) simplifies to

$$H(\omega, 0) = L(\omega) - L(\Omega_0) = 0 \quad (4)$$

and when $p = 1$, $H(\omega, p)$ as shown in Eq. (5):

$$H(\omega, 1) = L(\omega) + N(\omega) - F(v) = 0 \quad (5)$$

By incrementally adjusting p from 0 to 1, $\omega(v, p)$ transitions from the initial approximation $\Omega_0(v)$ to the exact solution $\Omega(v)$. This procedure is commonly known as deformation in topology, with $L(\omega) - L(\Omega_0)$ and $L(\omega) + N(\omega) - F(v)$ serving as the homotopy.

We solve Eqs. (2) and (3) by expanding the power series in terms of p .

$$\omega(\chi, \zeta) = \omega_0 + p\omega_1 + p^2\omega_2 + \dots \quad (6)$$

where p is a small parameter. By assigning $p = 1$ in Eq. (6), the solution approximating the original differential equation is obtained as

$$\Omega = \lim_{p \rightarrow 1} \omega = \omega_0 + \omega_1 + \omega_2 + \dots \quad (7)$$

The convergence of Eq. (7) is generally ensured under

certain conditions on the nonlinear operator N . Specifically, the series converges if the second derivative of $N(\omega)$ with respect to ω is small and if the norm of $L^{-1} \frac{\partial N}{\partial \omega}$ remains less than one.^[4] These conditions help control the rate of convergence, particularly when the embedding parameter p approaches unity. For a deeper exploration of HPM and its development.^[4, 22-26]

2.2 Padé approximants

The Padé approximation is a widely used technique to improve the convergence of a series solution. For a function $\phi(\xi)$, the Padé approximant of order $[\alpha/\beta]$ is defined as

$$\left[\frac{\alpha}{\beta} \right] (\xi) = \frac{p_\alpha(\xi)}{q_\beta(\xi)} = \frac{\sum_{i=0}^\alpha a_i \xi^i}{1 + \sum_{j=1}^\beta b_j \xi^j} \tag{8}$$

where $p_\alpha(\xi)$ and $q_\beta(\xi)$ are polynomials of degrees at most α and β , respectively. To avoid common factors in Eq. (8), the scaling condition $q_\beta(0) = 1$ is imposed. The series representation of $\phi(\xi)$ is expressed as

$$\phi(\xi) = \sum_{i=0}^\infty c_i \xi^i \tag{9}$$

The difference between the series expansion in Eq. (9) and the Padé approximant in Eq. (8) is given by

$$\phi(\xi) - \frac{p_\alpha(\xi)}{q_\beta(\xi)} = O(\xi^{\alpha+\beta+1}) \tag{10}$$

By multiplying the series by $q_\beta(\xi)$, a system of linear equations for the coefficients of $p_\alpha(\xi)$ and $q_\beta(\xi)$ is obtained

$$\begin{cases} c_{\alpha+1} + c_\alpha b_1 + \dots + c_{\alpha-\beta+1} b_\beta = 0 \\ c_{\alpha+2} + c_{\alpha+1} b_1 + \dots + c_{\alpha-\beta+2} b_\beta = 0 \\ \vdots \\ c_{\alpha+\beta} + c_{\alpha+\beta-1} b_1 + \dots + c_\alpha b_\beta = 0 \end{cases} \tag{11}$$

$$\begin{cases} c_0 = a_0 \\ c_0 + c_0 b_1 = a_1 \\ c_2 + c_1 b_1 + c_0 b_2 = a_2 \\ \vdots \\ c_\alpha + c_{\alpha-1} b_1 + \dots + c_0 b_\alpha = a_\alpha \end{cases} \tag{12}$$

The coefficients b_j are determined from Eq. (11), and the coefficients a_i follow accordingly from Eq. (12). Minimizing the error in Eq. (10) is achieved by ensuring that $\alpha + \beta + 1$ is constant, with the degrees of the numerator and denominator chosen for optimal accuracy. For additional details on Padé approximants.^[27,28]

2.3 Modified homotopy perturbation method

Many analytical and numerical methods provide power series solutions for nonlinear PDEs. However, truncated series often have limited convergence domains, making them impractical for highly nonlinear problems. To overcome this limitation, MHPM integrates the Laplace transform and Padé approximants, enhancing solution accuracy and convergence. The steps of MHPM are as follows

1. First, we obtain the 6-term series solution using the

HPM by expanding the solution as a power series and solving iteratively for each term.

2. Next, we extract the solution and express it in the form $\Omega_6(\chi, \zeta) = f(\zeta)g(\chi)$, where $f(\zeta)$ is formed by summing the relevant series terms.

3. The Laplace transform is applied to $f(\zeta)$, converting the differential equation into an algebraic form for easier manipulation.

4. We then substitute $s = \frac{1}{\zeta}$ to restructure the transformed series.

5. The Padé approximant of order $[2/2]$ is applied to the transformed function, converting the power series into a rational function to extend the solution's convergence domain.

6. We recall that $\zeta = \frac{1}{s}$, reversing the previous substitution to return the solution to its original domain.

7. Finally, the inverse Laplace transform is applied to retrieve the solution in its original form, yielding the exact solution for the nonlinear PDE.

This approach significantly enhances the classical HPM by accelerating convergence and eliminating divergence issues, making it highly effective for solving complex nonlinear PDEs in applied mathematics and engineering. The integration of Laplace transforms and Padé approximants ensures rapid approximation of the exact solution without requiring iterative corrections. Unlike traditional numerical techniques, MHPM does not rely on discretization, linearization, or small parameter assumptions, making it particularly suitable for strongly nonlinear problems. Additionally, it optimally balances accuracy and computational cost, reducing the number of terms required in the perturbation series while maintaining precision and minimizing computational effort.

Another important characteristic of MHPM is its versatility, as it applies to both real-valued and complex-valued nonlinear PDEs. This adaptability makes it useful across various disciplines, including fluid dynamics, wave mechanics, and quantum systems. The method also ensures solution stability even in strongly nonlinear or oscillatory cases by transforming the original equation into a more analytically manageable form, overcoming a common limitation of traditional perturbation methods. Furthermore, MHPM directly yields exact closed-form solutions for a wide range of nonlinear PDEs, eliminating the need for iterative refinements or approximations commonly required in numerical schemes. These properties establish MHPM as a powerful and efficient tool for addressing complex nonlinear systems, providing a significant improvement over conventional perturbation techniques.

3 Applications of MHPM

This section demonstrates the application of MHPM to several prominent nonlinear equations, showcasing its efficiency and simplicity. The results highlight the method's reliability and accuracy in addressing complex problems. Numerical outcomes for the Examples 1-6 are presented in Tables 1-6 and

Figs. 1-9. Throughout this section, the terms $\tilde{\Omega}_6, \Omega_E, E_\Omega, E_{Re(\Omega)}$, and $E_{Im(\Omega)}$ represent the six-term approximate solution obtained using HPM, the exact solution, the absolute error of Ω , the absolute error of the real part of Ω , and the absolute error of the imaginary part of Ω , respectively. These results underscore the effectiveness of MHPM in producing highly accurate solutions for a variety of nonlinear problems.

Example 1. Consider the nonlinear gas dynamic equation (Eq. (13))

$$\begin{cases} \Omega_\zeta + \Omega(\Omega_\chi + \Omega - 1) = 0 \\ \Omega(\chi, 0) = e^{-\chi} \end{cases} \quad (13)$$

By utilizing the homotopy technique, we construct Eq. (14):

$$\omega_\zeta - (\Omega_0)_\zeta + p[(\Omega_0)_\zeta + \omega(\omega_\chi + \omega - 1)] = 0 \quad (14)$$

Incorporate Eq. (5) into Eq. (13), match terms with identical powers of p , and derive the solution iteratively to obtain Eq. (15):

$$\begin{aligned} \omega_0(\chi, \zeta) &= e^{-\chi} + \zeta e^{-\chi}, & \omega_1(\chi, \zeta) &= \frac{1}{2} e^{-\chi} \zeta^2, \\ \omega_2(\chi, \zeta) &= \frac{1}{6} e^{-\chi} \zeta^3, & \omega_3(\chi, \zeta) &= \frac{1}{24} e^{-\chi} \zeta^4, \\ \omega_4(\chi, \zeta) &= \frac{1}{120} e^{-\chi} \zeta^5 \end{aligned} \quad (15)$$

The 6-term series solution obtained using HPM for Eq. (13) is

$$\begin{aligned} \tilde{\Omega}_6(\chi, \zeta, \tau) &= e^{-\chi} + \zeta e^{-\chi} + \frac{1}{2} e^{-\chi} \zeta^2 + \frac{1}{6} e^{-\chi} \zeta^3 + \\ &+ \frac{1}{24} e^{-\chi} \zeta^4 + \frac{1}{120} e^{-\chi} \zeta^5 = \left(1 + \zeta + \frac{\zeta^2}{2} + \frac{\zeta^3}{6} + \frac{\zeta^4}{24} + \frac{\zeta^5}{120}\right) e^{-\chi} = \\ &= f(\zeta) e^{-\chi} \end{aligned} \quad (16)$$

where $f(\zeta) = 1 + \zeta + \frac{\zeta^2}{2} + \frac{\zeta^3}{6} + \frac{\zeta^4}{24} + \frac{\zeta^5}{120}$. Taking the Laplace transform of f with respect to ζ results in Eq. (17):

$$\mathcal{L}[f(\zeta)] = \frac{s^5 + s^4 + s^3 + s^2 + s + 1}{s^6} \quad (17)$$

Substituting $s = \frac{1}{\zeta}$, the equation above takes the form Eq. (18):

$$\mathcal{L}[f(\zeta)] = \zeta^6 + \zeta^5 + \zeta^4 + \zeta^3 + \zeta^2 + \zeta \quad (18)$$

Using the Padé approximants, we get Eq. (19):

$$\left[\frac{2}{2} \right] (\zeta) = \frac{\zeta}{1-\zeta} \quad (19)$$

Recall that $\zeta = \frac{1}{s}$, and we have Eq. (20):

$$\left[\frac{2}{2} \right] (\zeta) = \frac{1}{s-1} \quad (20)$$

Finally, we perform the inverse Laplace transform on Eq. (20), obtaining $f(\chi) = e^\chi$. Plugging this result into Eq. (16), we achieve Eq. (21):

$$\Omega(\chi, \zeta) = e^{\zeta-\chi} \quad (21)$$

This result corresponds to the closed-form solution of Eq. (13).

Table 1: Numerical result of Example 1.

$\chi = \zeta$	$\tilde{\Omega}_6$	Ω_E	E_Ω
0	1	1	0
0.2	0.9999999251	1	7.49×10^{-8}
0.4	0.9999959573	1	4.04×10^{-6}
0.6	0.9999611439	1	3.89×10^{-5}
0.8	0.9998156575	1	1.84×10^{-4}
1	0.9994058152	1	5.94×10^{-4}

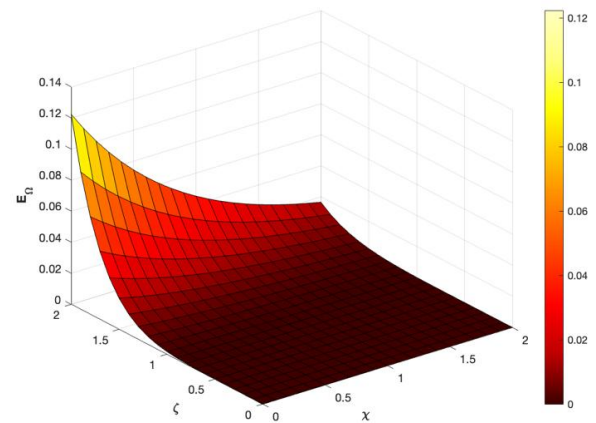


Fig. 1: Surface plot in 3D for E_Ω in Example 1.

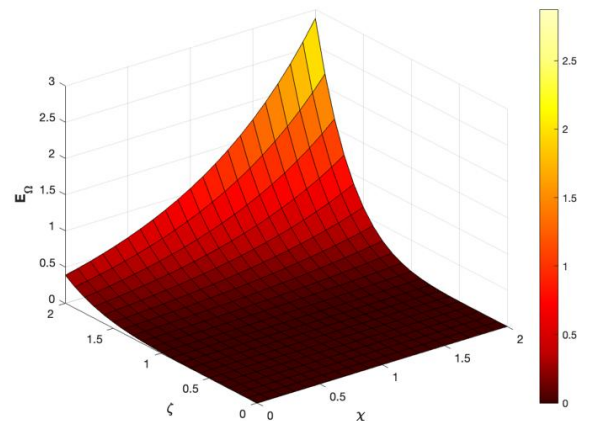


Fig. 2: Surface plot in 3D for E_Ω in Example 2.

Example 2. Consider the following nonlinear wave-like equation Eq. (22):

$$\begin{cases} \Omega_\zeta + \Omega^2 - \Omega_{\chi\chi} - \Omega\Omega_\chi - \Omega = 0 \\ \Omega(\chi, 0) = 1 + e^\chi \end{cases} \quad (22)$$

By utilizing the homotopy technique, we construct Eq. (23):

$$\omega_\zeta - (\Omega_0)_\zeta + p[(\Omega_0)_\zeta - \omega_{\chi\chi} - \omega\omega_\chi - \omega + \omega^2] = 0 \quad (23)$$

The 6-term series solution obtained using HPM for Eq. (22)

is in Eq. (24):

$$\tilde{\Omega}_6(\chi, \zeta) = 1 + e^\chi \left(1 + \zeta + \frac{\zeta^2}{2} + \frac{\zeta^3}{6} + \frac{\zeta^4}{24} \right) = 1 + f(\zeta)e^\chi \quad (24)$$

where $f(\zeta) = 1 + \zeta + \frac{\zeta^2}{2} + \frac{\zeta^3}{6} + \frac{\zeta^4}{24}$. Following a similar approach as in the earlier example, taking the Laplace transform of f with respect to ζ , followed by the substitution $s = \frac{1}{\zeta}$, results in Eq. (25):

$$\ell[f(\zeta)] = \zeta^5 + \zeta^4 + \zeta^3 + \zeta^2 + \zeta \quad (25)$$

Using the Padé approximants and recalling $\zeta = \frac{1}{s}$, we have Eq. (26):

$$\left[\frac{2}{2} \right] (\zeta) = \ell[f(\zeta)] = \frac{1}{s-1} \quad (26)$$

Finally, we perform ℓ^{-1} on Eq. (26), which yields Eq. (27):

$$f(\zeta) = e^\zeta \quad (27)$$

Plugging this result into Eq. (24), we achieve

$$\Omega(\chi, \zeta) = 1 + e^{\chi+\zeta} \quad (28)$$

This result corresponds to the closed-form solution of Eq. (28).

Table 2: Numerical result of Example 2.

$\chi = \zeta$	$\tilde{\Omega}_6$	Ω_E	E_Ω
0	2	2	0
0.2	2.4918213288	2.4918246976	3.37×10^{-6}
0.4	3.2254046290	3.2255409285	1.36×10^{-4}
0.6	4.3188071830	4.3201169227	1.31×10^{-3}
0.8	5.9460421595	5.9530324244	6.99×10^{-3}
1	8.3620132854	8.3890560989	2.70×10^{-2}

Example 3. Consider the following nonlinear cubic complex Ginzburg-Landau equation (Eq. (29)).

$$\begin{cases} \Omega_\zeta + (9i - 1)\Omega_{\chi\chi} - \frac{10}{9}\Omega + (1 - i)|\Omega|^2\Omega = 0 \\ \Omega(\chi, 0) = e^{-\frac{i}{3}\chi} \end{cases} \quad (29)$$

By utilizing the homotopy technique, we construct Eq. (30):

$$\omega_\zeta - (\Omega_0)_\zeta + p \left[(\Omega_0)_\zeta + (9i - 1)\omega_{\chi\chi} - \frac{10}{9}\omega + (1 - i)\bar{\omega}\omega^2 \right] = 0 \quad (30)$$

where $|\omega|^2\omega = \bar{\omega}\omega^2$ and $\bar{\omega}$ is the conjugate of ω . The 6-term series solution obtained using HPM for Eq. (29) is Eq. (31):

$$\tilde{\Omega}_6(\chi, \zeta) = \left(1 + 2i\zeta - 2\zeta^2 - \frac{4i\zeta^3}{3} + \frac{2\zeta^4}{3} + \frac{4i\zeta^5}{15} \right) e^{-\frac{i}{3}\chi} = f(\zeta)e^{-\frac{i}{3}\chi} \quad (31)$$

where $f(\zeta) = 1 + 2i\zeta - 2\zeta^2 - \frac{4i\zeta^3}{3} + \frac{2\zeta^4}{3} + \frac{4i\zeta^5}{15}$. Following a

similar approach as in the earlier examples, taking the Laplace transform of f with respect to ζ , followed by the substitution $s = \frac{1}{\zeta}$, results in Eq. (32):

$$\ell[f(\zeta)] = 32i\zeta^6 + 16\zeta^5 - 8i\zeta^4 - 4\zeta^3 + 2i\zeta^2 + \zeta \quad (32)$$

Using the Padé approximants, and recalling $\zeta = \frac{1}{s}$, we have Eq. (33):

$$\left[\frac{2}{2} \right] (\zeta) = \frac{1}{s-2i} \quad (33)$$

Finally, we perform ℓ^{-1} on Eq. (33), which yields Eq. (34):

$$f(\zeta) = e^{2i\zeta} \quad (34)$$

Plugging this result into Eq. (31), we achieve Eq. (35):

$$\Omega(\chi, \zeta) = e^{\frac{i}{3}(6\zeta-\chi)} \quad (35)$$

This result corresponds to the closed-form solution of Eq. (29).

Example 4. Consider the following nonlinear Schrödinger equation (Eq. (36)).

$$\begin{cases} i\Omega_\zeta + \Omega_{\chi\chi} + 6|\Omega|^2\Omega = 0 \\ \Omega(\chi, 0) = e^{3i\chi} \end{cases} \quad (36)$$

By utilizing the homotopy technique, we construct Eq. (37):

$$\omega_\zeta - (\Omega_0)_\zeta + p \left[(\Omega_0)_\zeta - i(\omega_{\chi\chi} + 6\bar{\omega}\omega^2) \right] = 0 \quad (37)$$

Table 3: Numerical result of Example 3.

$\chi = \zeta$	$\tilde{\Omega}_6$	Ω_E	E_Ω	
			$E_{\text{Re}(\Omega)}$	$E_{\text{Im}(\Omega)}$
0	1	1	0	0
0.2	0.94496262 + 0.32719464i	0.94495694 + 0.32719469i	5.68×10^{-6}	5.43×10^{-8}
0.4	0.78624950 + 0.61836282i	0.78588726 + 0.61836980i	3.62×10^{-4}	6.98×10^{-6}
0.6	0.54440243 + 0.84135093i	0.54030230 + 0.84147098i	4.10×10^{-3}	1.20×10^{-4}
0.8	0.25807151 + 0.97102972i	0.23523757 + 0.97193790i	2.28×10^{-2}	9.08×10^{-4}
1	-0.0096039 + 0.99102471i	-0.0957235 + 0.99540795i	8.61×10^{-2}	4.38×10^{-3}

The 6-term series solution obtained using HPM for Eq. (36) is Eq. (38):

$$\tilde{\Omega}_6(\chi, \zeta) = \left(1 - 3i\zeta - \frac{9\zeta^2}{2} + \frac{9i\zeta^3}{2} + \frac{27\zeta^4}{8} - \frac{81i\zeta^5}{40} \right) e^{3i\chi} = f(\zeta)e^{3i\chi} \quad (38)$$

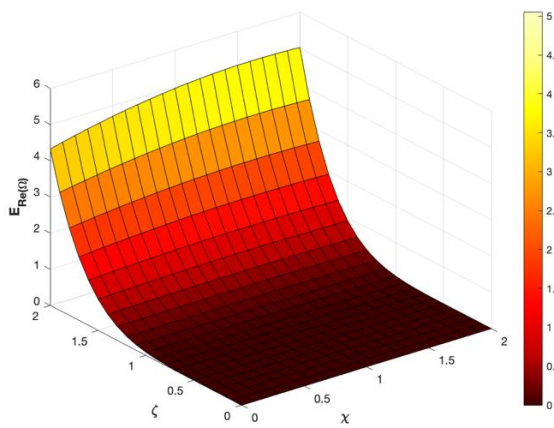


Fig. 3: Surface plot in 3D for $E_{Re(\Omega)}$ in Example 3.

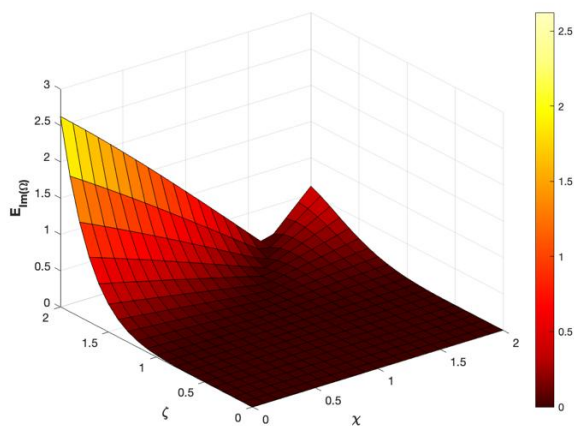


Fig. 4: Surface plot in 3D for $E_{Im(\Omega)}$ in Example 3.

where $f(\zeta) = 1 - 3i\zeta - \frac{9\zeta^2}{2} + \frac{9i\zeta^3}{2} + \frac{27\zeta^4}{8} - \frac{81i\zeta^5}{40}$. Following a similar approach as in the earlier examples, taking the Laplace transform of f with respect to ζ , followed by the substitution $s = \frac{1}{\zeta}$, results in Eq. (39):

$$\ell[f(\zeta)] = -243i\zeta^6 + 81\zeta^5 + 27i\zeta^4 - 9\zeta^3 - 3i\zeta^2 + \zeta \quad (39)$$

Using the Padé approximants, and recalling $\zeta = \frac{1}{s}$, we have Eq. (40):

$$\left[\frac{2}{2} \right] (\zeta) = \frac{1}{s+3i} \quad (40)$$

Finally, we perform ℓ^{-1} on Eq. (40), which yields Eq. (41):

$$f(\zeta) = e^{-3i\zeta} \quad (41)$$

Plugging this result into Eq. (38), we achieve Eq. (42):

$$\Omega(\chi, \zeta) = e^{3i(\chi-\zeta)} \quad (42)$$

This result corresponds to the closed-form solution of Eq. (36).

Example 5. Consider the following two-dimensional nonlinear Schrödinger equation

Table 4: Numerical result of Example 4.

$\tau = \zeta$	$\tilde{\Omega}_6$	Ω_E	E_Ω	
			$E_{Re(\Omega)}$	$E_{Im(\Omega)}$
0	1	1	0	0
0.2	1.0000562599 + 0.0000317933i	1	5.63 $\times 10^{-5}$	3.18 $\times 10^{-5}$
0.4	1.0021142901 + 0.0035149986i	1	2.11 $\times 10^{-3}$	3.51 $\times 10^{-3}$
0.6	1.0011788842 + 0.0460749076i	1	1.18 $\times 10^{-3}$	4.61 $\times 10^{-2}$
0.8	0.8799765226 + 0.2239783928i	1	1.20 $\times 10^{-1}$	2.24 $\times 10^{-1}$
1	0.1978370663 + 0.5021060597i	1	8.02 $\times 10^{-1}$	5.02 $\times 10^{-1}$

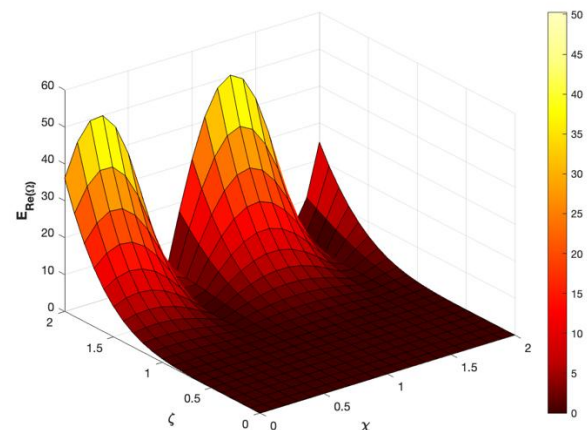


Fig. 5: Surface plot in 3D for $E_{Re(\Omega)}$ in Example 4.

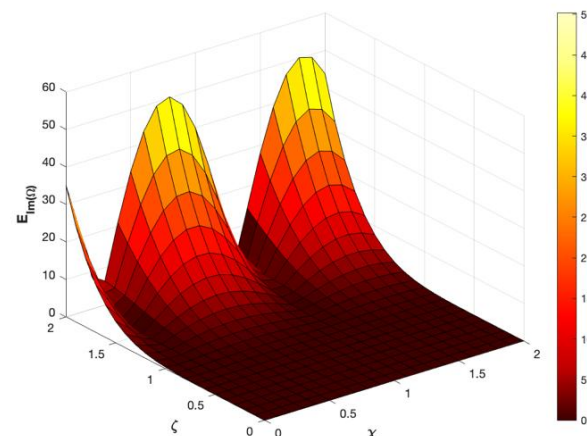


Fig. 6: Surface plot in 3D for $E_{Im(\Omega)}$ in Example 4.

$$\begin{cases} i\Omega_\tau + \frac{1}{2}(\Omega_{\chi\chi} + \Omega_{\zeta\zeta}) + (\sin^2 \chi \sin^2 \zeta - 1)\Omega - |\Omega|^2\Omega = 0 \\ \Omega(\chi, \zeta, 0) = \sin \chi \sin \zeta \end{cases} \quad (43)$$

By utilizing the homotopy technique, we construct Eq. (44)

$$\omega_\tau - (\Omega_0)_\tau + p \left[(\Omega_0)_\tau - i \left(\frac{1}{2}(\omega_{\chi\chi} + \omega_{\zeta\zeta}) + (\sin^2 \chi \sin^2 \zeta - 1)\omega - |\omega|^2\omega \right) \right] = 0 \quad (44)$$

The 6-term series solution obtained using HPM for Eq. (43) is Eq. (45):

$$\tilde{\Omega}_6(\chi, \zeta, \tau) = \sin \chi \sin \zeta \left(1 - 2i\tau - 2\tau^2 - \frac{4i\tau^3}{3} + \frac{2\tau^4}{3} + \frac{4i\tau^5}{15} \right) = \sin \chi \sin \zeta f(\tau) \quad (45)$$

where $f(\tau) = 1 - 2i\tau - 2\tau^2 - \frac{4i\tau^3}{3} + \frac{2\tau^4}{3} + \frac{4i\tau^5}{15}$. Following a similar approach as in the earlier examples, taking the Laplace transform of f with respect to τ , followed by the substitution $s = \frac{1}{\tau}$, results in Eq. (46):

$$\ell[f(\tau)] = 32i\tau^6 + 16\tau^5 - 8i\tau^4 - 4\tau^3 - 2i\tau^2 + \tau \quad (46)$$

Using the Padé approximants, and recalling $\tau = \frac{1}{s}$, we have Eq. (47):

$$\left[\frac{2}{2} \right] (\tau) = \frac{1}{s+2i} \quad (47)$$

Finally, we perform ℓ^{-1} on Eq. (47), which yields Eq. (48):

$$f(\tau) = e^{-2i\tau} \quad (48)$$

Plugging this result into Eq. (45), we achieve Eq. (49):

$$\Omega(\chi, \zeta, \tau) = \sin \chi \sin \zeta e^{-2i\tau} \quad (49)$$

This result corresponds to the closed-form solution of Eq. (43).

Table 5: Numerical result of Example 5.

χ $= \zeta$ $= \tau$	$\tilde{\Omega}_6$	Ω_E	E_Ω	
			$E_{Re(\Omega)}$	$E_{Im(\Omega)}$
0	0	0	0	0
0.2	0.03635404 - 0.01620544i	0.03635381 - 0.01537014i	2.24 $\times 10^{-7}$	8.35 $\times 10^{-4}$
0.4	0.10570782 - 0.13384373i	0.10565324 - 0.10878464i	5.46 $\times 10^{-5}$	2.51 $\times 10^{-2}$
0.6	0.11681606 - 0.46779476i	0.11552731 - 0.29715375i	1.29 $\times 10^{-3}$	1.71 $\times 10^{-1}$
0.8	-0.00356789- 1.12969331i	-0.01502607 - 0.51438034i	1.15 $\times 10^{-2}$	6.15 $\times 10^{-1}$
1	-0.23602447- 2.17142515i	-0.29466251- 0.64384934i	5.86 $\times 10^{-2}$	1.53

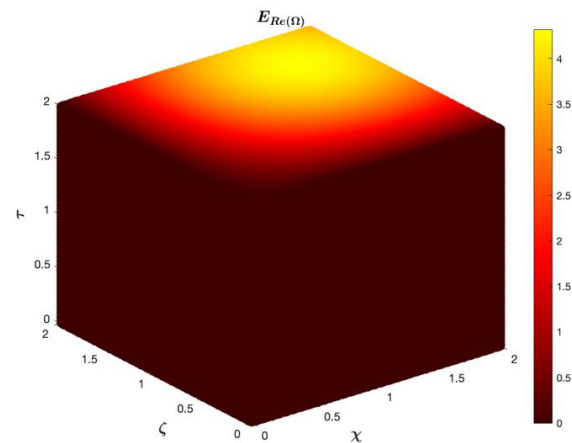


Fig. 7: Scatter plot in 3D for $E_{Re(\Omega)}$ in Example 5.

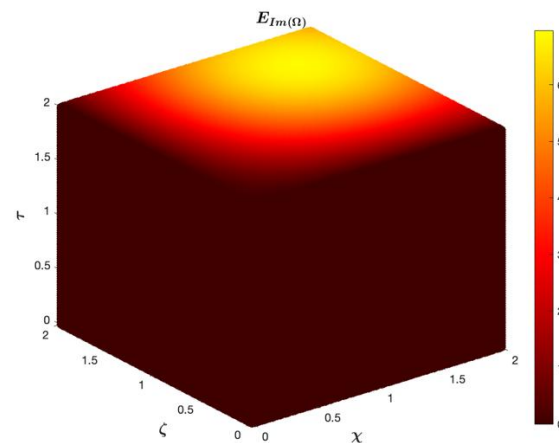


Fig. 8: Scatter plot in 3D for $E_{Im(\Omega)}$ in Example 5.

Example 6. Consider the following higher-order nonlinear PDE in Eq. (50).

$$\begin{cases} \Omega_{\chi\chi\chi} - \Omega_{\chi\zeta\zeta} - \Omega_{\zeta\zeta\chi\chi} + \Omega_{\zeta\zeta\zeta\zeta} - \Omega_\chi - \Omega_{\chi\chi}\Omega_\zeta = 0 \\ \Omega(0, \zeta) = \cos \zeta \\ \Omega_\chi(0, \zeta) = -\sin \zeta \\ \Omega_{\chi\chi}(0, \zeta) = -\cos \zeta \end{cases} \quad (50)$$

By utilizing the homotopy technique, we construct Eq. (51):

$$\omega_{\chi\chi\chi} - (\Omega_0)_{\chi\chi\chi} + p \left[(\Omega_0)_{\chi\chi\chi} - \omega_{\chi\zeta\zeta} - \omega_{\zeta\zeta\chi\chi} + \omega_{\zeta\zeta\zeta\zeta} - \omega\omega_\chi - \omega_{\chi\chi}\omega_\zeta \right] = 0 \quad (51)$$

The 6-term series solution obtained using HPM for Eq. (45) is Eq. (52):

$$\tilde{\Omega}_6(\chi, \zeta) = \cos \zeta \left(1 - \frac{\chi^2}{2} + \frac{\chi^4}{24} \right) - \sin \zeta \left(\chi - \frac{\chi^3}{6} + \frac{\chi^5}{120} \right) \quad (52)$$

where $f(\chi) = 1 - \frac{\chi^2}{2} + \frac{\chi^4}{24}$ and $g(\chi) = \chi - \frac{\chi^3}{6} + \frac{\chi^5}{120}$.

Following a similar approach as in the earlier examples, taking the Laplace transform of f and g with respect to χ , followed by the substitution $s = \frac{1}{\chi}$, results in Eq. (53):

$$\begin{cases} \ell[f(\chi)] = \chi^5 - \chi^3 + \chi \\ \ell[g(\chi)] = \chi^6 - \chi^4 + \chi^2 \end{cases} \quad (53)$$

Using the Padé approximants, and recalling $\chi = \frac{1}{s}$, we have Eq. (54):

$$\left[\begin{matrix} 2 \\ 2 \end{matrix} \right] (\chi) = \begin{cases} \ell[f(\chi)] = \frac{1}{s+2i} \\ \ell[g(\chi)] = \frac{1}{s^2+1} \end{cases} \quad (54)$$

Finally, we perform ℓ^{-1} on Eq. (54), which yields Eq. (55):

$$\begin{cases} f(\chi) = \cos \chi \\ g(\chi) = \sin \chi \end{cases} \quad (55)$$

Plugging this result into Eq. (52), we achieve Eq. (56):

$$\Omega(\chi, \zeta) = \cos \zeta \cos \chi - \sin \zeta \sin \chi = \cos(\zeta + \chi) \quad (56)$$

This result corresponds to the closed-form solution of Eq. (50).

Table 6: Numerical result of Example 6.

$\chi = \zeta$	$\tilde{\Omega}_6$	Ω_E	E_Ω
0	1	1	0
0.2	0.9210610806	0.9210609940	8.66×10^{-8}
0.4	0.6967118079	0.6967067093	5.10×10^{-6}
0.6	0.3624077732	0.3623577545	5.00×10^{-5}
0.8	-	-	2.21×10^{-4}
1	0.0289783231	0.0291995223	
	-	-	5.73×10^{-4}
	0.4155743299	0.4161468365	

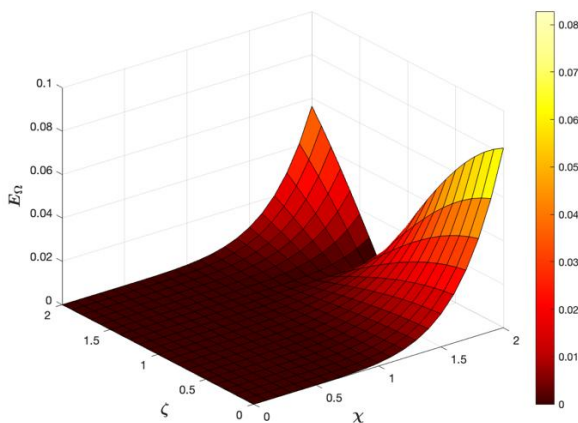


Fig. 9: Surface plot in 3D for E_Ω in Example 6.

4. Results and discussion

By applying MHPM to widely studied nonlinear PDEs, this study demonstrates its capability and computational efficiency, setting it apart from traditional methods such as HPM. The findings underscore MHPM's ability to deliver exact solutions, effectively addressing the shortcomings of conventional numerical techniques. The numerical results are summarized in Tables 1-6 and Figs. 1-9, comparing the six-term

approximate solutions obtained using HPM with the exact solutions, which are the same solutions generated by MHPM. This demonstrates the precision and robustness of the method, even for highly nonlinear or complex-valued equations.

As the variables χ, ζ , and τ increase in magnitude, the approximation provided by HPM begins to lose accuracy, as reflected in the growing absolute error (E_Ω). This decline underscores the limitations of HPM in maintaining precision for larger values of these variables. In contrast, MHPM consistently delivers exact solutions, regardless of the variable range, showcasing its ability to handle complex systems without degradation in accuracy. This distinction is evident in the accompanying figures, which illustrate the steady rise in absolute error for HPM as χ, ζ , and τ increase, underscoring MHPM's precision. The corresponding tables provide a detailed numerical perspective, comparing the analytical solutions produced by MHPM with the 6-term series solutions from HPM and highlighting the errors, offering clear evidence of MHPM's superior performance.

A significant advantage of MHPM is its ability to address challenges typically encountered in solving nonlinear PDEs, such as strong nonlinearities, oscillatory behaviors, and interactions between variables. Employing Laplace transforms alongside Padé approximants, the method effectively enhances the convergence of the solution series, enabling it to directly reach the exact solution without requiring iterative corrections or approximations. This is evident in all examples, where MHPM efficiently resolves the nonlinearities inherent in the equations while maintaining computational simplicity.

The versatility of MHPM is evident in its application to both real-valued and complex-valued equations. For instance, the nonlinear cubic complex Ginzburg-Landau equation and the nonlinear Schrödinger equations, which involve intricate interactions between real and imaginary components, are solved precisely using the method. Similarly, equations with exponential or oscillatory solutions (such as the nonlinear gas dynamics and wave-like equations) are handled seamlessly, further validating MHPM's reliability and flexibility.

While MHPM delivers remarkable results in the examples discussed, certain limitations of the current analysis should be noted. This work emphasizes certain categories of PDEs that feature relatively straightforward boundary conditions. Addressing more intricate boundary configurations or systems in higher dimensions may necessitate further adjustments to MHPM to ensure its precision and effectiveness. Moreover, although the method exhibits notable efficiency for the examples considered, its applicability to particularly stiff systems remains an open area of exploration, potentially requiring additional refinements. Numerical computations and graphical results were obtained using MATLAB to implement MHPM.

5. Conclusion

This study presents MHPM as a highly effective approach for solving nonlinear partial differential equations (PDEs). By

incorporating Laplace transforms and Padé approximants into the traditional HPM, MHPM addresses key challenges such as slow convergence, instability, and computational inefficiency, which often limit conventional analytical and numerical techniques. The method successfully produces exact solutions for a range of nonlinear PDEs, including those fundamental to fluid dynamics, wave propagation, and quantum mechanics, demonstrating its versatility in handling both real and complex domains.

A systematic comparison highlights MHPM's advantages over standard perturbation methods, showing its ability to maintain accuracy across a broad spectrum of problems without requiring additional corrections or iterative refinements. The numerical results, validated against known analytical solutions, confirm that MHPM consistently delivers precise solutions while significantly reducing computational effort.

Beyond its demonstrated effectiveness, MHPM opens new possibilities for tackling more complex multi-dimensional and time-dependent PDEs. Future research can explore its integration with numerical methods to enhance its applicability to computationally intensive problems. This study establishes MHPM as a powerful and reliable tool for advancing the study of nonlinear systems, offering a precise, computationally efficient, and adaptable framework for solving challenging equations in applied mathematics, physics, and engineering.

This study presents MHPM as a highly effective approach for solving nonlinear partial differential equations (PDEs). By incorporating Laplace transforms and Padé approximants into the traditional HPM, MHPM addresses key challenges such as slow convergence, instability, and computational inefficiency, which often limit conventional analytical and numerical techniques. The method successfully produces exact solutions for a range of nonlinear PDEs, including those fundamental to fluid dynamics, wave propagation, and quantum mechanics, demonstrating its versatility in handling both real and complex domains.

A systematic comparison highlights MHPM's advantages over standard perturbation methods, showing its ability to maintain accuracy across a broad spectrum of problems without requiring additional corrections or iterative refinements. The numerical results, validated against known analytical solutions, confirm that MHPM consistently delivers precise solutions while significantly reducing computational effort.

Beyond its demonstrated effectiveness, MHPM opens new possibilities for tackling more complex multi-dimensional and time-dependent PDEs. Future research can explore its integration with numerical methods to enhance its applicability to computationally intensive problems. This study establishes MHPM as a powerful and reliable tool for advancing the study of nonlinear systems, offering a precise, computationally efficient, and adaptable framework for solving challenging equations in applied mathematics, physics,

and engineering. Its relevance is further underscored by practical applications such as modeling fluid flows in aerodynamics, analyzing optical transmission in photonics, and simulating quantum transport phenomena in nanoscale systems.

Conflict of Interest

There is no conflict of interest.

Supporting Information

Not applicable.

References

- [1] G. Adomian, Solving Frontier Problems of Physics: The Decomposition Method, Kluwer, Boston, 1994.
- [2] J. He, Variational iteration method for delay differential equations, *Communications in Nonlinear Science and Numerical Simulation*, 1997, **2**, 235-236, doi: 10.1016/s1007-5704(97)90008-3.
- [3] J. He, Some asymptotic methods for strongly nonlinear equations, *International Journal of Modern Physics B*, 2006, **20**, 1141-1199, doi: 10.1142/s0217979206033796.
- [4] J. He, Homotopy perturbation technique, *Computer Methods in Applied Mechanics and Engineering*, 1999, **178**, 257-262, doi: 10.1016/s0045-7825(99)00018-3.
- [5] M. B. Almatrafi, Solitary wave solutions to a fractional-order fokas equation via the improved modified extended tanh-function approach, *Mathematics*, 2025, **13**, 109, doi: 10.3390/math13010109.
- [6] M. B. Almatrafi, Solitary wave solutions to a fractional model using the improved modified extended tanh-function method, *Fractal and Fractional*, 2023, **7**, 252, doi: 10.3390/fractalfract7030252.
- [7] M. B. Almatrafi, Abundant traveling wave and numerical solutions for Novikov-Veselov system with their stability and accuracy, *Applicable Analysis*, 2023, **102**, 2389-2402, doi: 10.1080/00036811.2022.2027381.
- [8] M. B. Almatrafi, Construction of closed form soliton solutions to the space-time fractional symmetric regularized long wave equation using two reliable methods, *Fractals*, 2023, **31**, 2340160, doi: 10.1142/s0218348x23401606.
- [9] M. Berkal, M. B. Almatrafi, Bifurcation and stability of two-dimensional activator-inhibitor model with fractional-order derivative, *Fractal and Fractional*, 2023, **7**, 344, doi: 10.3390/fractalfract7050344.
- [10] S. Djennadi, N. Shawagfeh, O. Abu Arqub, A numerical algorithm in reproducing kernel-based approach for solving the inverse source problem of the time-space fractional diffusion equation, *Partial Differential Equations in Applied Mathematics*, 2021, **4**, 100164, doi: 10.1016/j.padiff.2021.100164.
- [11] O. Abu Arqub, Numerical solutions for the Robin time-fractional partial differential equations of heat and fluid flows based on the reproducing kernel algorithm, *International Journal of Numerical Methods for Heat & Fluid Flow*, 2018, **28**, 828-856,

doi: 10.1108/hff-07-2016-0278.

- [12] O. Abu Arqub, Computational algorithm for solving singular Fredholm time-fractional partial integrodifferential equations with error estimates, *Journal of Applied Mathematics and Computing*, 2019, **59**, 227-243, doi: 10.1007/s12190-018-1176-x.
- [13] W. Beghami, B. Maayah, S. Bushnaq, O. Abu Arqub, The Laplace optimized decomposition method for solving systems of partial differential equations of fractional order, *International Journal of Applied and Computational Mathematics*, 2022, **8**, 52, doi: 10.1007/s40819-022-01256-x.
- [14] J. Al-Saif, D. A. Abood, The Homotopy perturbation method for solving K(2,2) equation, *AIP Conference Proceedings*, 2019, **2142**, 030007.
- [15] A. A. Hemed, Modified Homotopy perturbation method for solving fractional differential equations, *Journal of Applied Mathematics*, 2023, **2014**, 594245, doi: 10.1155/2014/594245.
- [16] J. H. He, Comparison of Homotopy perturbation method and Homotopy analysis method, *Applied Mathematics and Computation*, 2004, **156**, 527-539, doi: 10.1016/j.amc.2003.08.008.
- [17] L. Xu, He's Homotopy perturbation method for a boundary layer equation in unbounded domain, *Computers & Mathematics with Applications*, 2007, **54**, 1067-1070, doi: 10.1016/j.camwa.2006.12.052.
- [18] O. Alkhazaleh, O. Ala'yed, A study of solutions for some classes of PDEs arising in physics and engineering using modified reduced differential transform method, *Journal of Applied Mathematics*, 2025, **2025**, 6866952, doi: 10.1155/jama/6866952.
- [19] O. Alkhazaleh, Modification of Homotopy Perturbation method for addressing systems of PDEs, *Partial Differential Equations in Applied Mathematics*, 2025, **13**, 101065, doi: 10.1016/j.padiff.2024.101065.
- [20] O. Ala'yed, A. Qazza, R. Saadeh, O. Alkhazaleh, A quintic B-spline technique for a system of Lane-Emden equations arising in theoretical physical applications, *AIMS Mathematics*, 2024, **9**, 4665-4683, doi: 10.3934/math.2024225.
- [21] S. Momani, G. H. Erjaee, M. H. Alnasr, The modified Homotopy perturbation method for solving strongly nonlinear oscillators, *Computers & Mathematics with Applications*, 2009, **58**, 2209-2220, doi: 10.1016/j.camwa.2009.03.082.
- [22] J. He, A coupling method of a Homotopy technique and a perturbation technique for non-linear problems, *International Journal of Non-Linear Mechanics*, 2000, **35**, 37-43, doi: 10.1016/s0020-7462(98)00085-7.
- [23] J. He, Recent developments of the Homotopy perturbation method, *Topological Methods in Nonlinear Analysis*, 2008, **31**, 205-209.
- [24] J. He, An elementary introduction to the Homotopy perturbation method, *Computers & Mathematics with Applications*, 2009, **57**, 410-412, doi: 10.1016/j.camwa.2008.06.003.
- [25] S. Liao, An approximate solution technique not depending on small parameters: A special example, *International Journal of Non-Linear Mechanics*, 1995, **30**, 371-380, doi: 10.1016/0020-

7462(94)00054-E.

- [26] S. J. Liao, Beyond Perturbation: Introduction to Homotopy Analysis Method, CRC Press, Boca Raton, 2004.
- [27] G. A. Baker, Essentials of Padé Approximants, Academic Press, San Diego, 1975.
- [28] B. Benhammouda, H. Vazquez-Leal, A. Sarmiento-Reyes, Modified reduced differential transform method for partial differential-algebraic equations, *Journal of Applied Mathematics*, 2014, **2014**, 279481, doi: 10.1155/2014/279481.

Publisher's Note: Engineered Science Publisher remains neutral with regard to jurisdictional claims in published maps and institutional affiliations.

Open Access

This article is licensed under a Creative Commons Attribution 4.0 International License, which permits the use, sharing, adaptation, distribution and reproduction in any medium or format, as long as appropriate credit to the original author(s) and the source is given by providing a link to the Creative Commons license and changes need to be indicated if there are any. The images or other third-party material in this article are included in the article's Creative Commons license, unless indicated otherwise in a credit line to the material. If material is not included in the article's Creative Commons license and your intended use is not permitted by statutory regulation or exceeds the permitted use, you will need to obtain permission directly from the copyright holder. To view a copy of this license, visit <http://creativecommons.org/licenses/by/4.0/>.

©The Author(s) 2025